

Boosting Large Language Models with Mask Fine-Tuning

Mingyuan Zhang^{*1} Yue Bai^{*1} Huan Wang¹ Yizhou Wang¹ Qihua Dong¹ Yun Fu^{1,2}

Abstract

The model is usually kept integral in the mainstream large language model (LLM) fine-tuning protocols. No works have questioned whether maintaining the integrity of the model is *indispensable* for performance. In this work, we introduce *Mask Fine-Tuning* (MFT), a brand-new LLM fine-tuning paradigm to show that properly *breaking* the integrity of the model can surprisingly lead to improved performance. Specifically, MFT learns a set of binary masks supervised by the typical LLM fine-tuning objective. Extensive experiments show that MFT gains a consistent performance boost across various domains and backbones (e.g., 1.95% / 1.88% average gain in coding with LLaMA2-7B / 3.1-8B). Detailed procedures are provided to study the proposed MFT from different hyperparameter perspectives for better insight. In particular, MFT naturally updates the current LLM training protocol by deploying it on a complete well-trained model. This study extends the functionality of mask learning from its conventional network pruning context for model compression to a more general scope.

1. Introduction

Pre-training large language model (LLM) typically requires massive corpora to enable models with foundational knowledge and linguistic competencies for effective language generation (Radford et al., 2019; Brown et al., 2020; Touvron et al., 2023; Dubey et al., 2024). After this, the pre-trained LLMs are transferred to downstream tasks by specific fine-tuning using high-quality domain data, which includes specialized knowledge such as math and coding (Cobbe et al., 2021; Yu et al., 2023; Chen et al., 2021; Austin et al., 2021), or particular patterns such as human instruction (Zhou et al., 2023a; Dubois et al., 2024). For such adap-

^{*}Equal contribution ¹Department of ECE, College of Engineering, Northeastern University, Boston, USA ²Khoury College of Computer Science, Northeastern University, Boston, USA. Correspondence to: Yue Bai <bai.yue@northeastern.edu>.

Preprint version. Code available at: <https://github.com/Ming-K9/MFT>

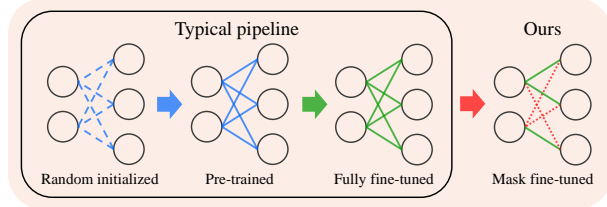


Figure 1. Typical LLM training contains pre-training and fine-tuning for foundation capacity and domain knowledge, where the LLM structure is always kept entirely. We are curious if such integrity is necessary for good performance and propose MFT to generally outperform model with sufficient FFT. Therefore, MFT naturally upgrades the classic fine-tuning pipeline by following typical protocol to further refine well-optimized LLMs.

tation, fine-tuning all model parameters is the most common method, commonly referred to as full fine-tuning (FFT), which generally achieves the most competitive performance. Furthermore, adapter-based alternatives offer a parameter-efficient fine-tuning (PEFT) strategy (e.g., vanilla bottleneck adapters (Houlsby et al., 2019) and LoRA (Hu et al., 2021)). These methods fix the pre-trained backbone and introduce a limited number of learnable parameters, which makes them well suited to scenarios with limited computational budget, especially for insufficient fine-tuning data. However, they may sacrifice fine-tuning performance gain compared with FFT. Overall, this pipeline of language model pre-training followed by fine-tuning has demonstrated promising results across a range of language tasks, including domains requiring extensive specialized knowledge (e.g., medicine (Wang et al., 2023) and law (Nguyen, 2023)) and complex reasoning (e.g., math (Frieder et al., 2024) and coding (Chen et al., 2021)), exhibiting remarkably intelligent capabilities.

However, these mainstream fine-tuning strategies (FFT and PEFT), benchmarking the strong baseline of LLM fine-tuning, both treat the language model structure as a whole, where FFT optimizes all its parameters simultaneously and PEFT freezes it to tune additional adapter parameters. In other words, both accept the necessity of LLM structural integrity by default. Such practice naturally inspires us to ask: *is such structural integrity indispensable for good model performance?*, or even further, is there potential to further improve the model by removing certain model components which breaks the structural integrity?

We propose a mask fine-tuning (MFT) to answer this question in this study. Starting from a well-trained LLM (model after sufficient FFT in our study), MFT freezes this given LLM and learns a binary mask on it. Specifically, we use the common LLM fine-tuning supervision to guide the mask learning, leveraging on the straight-through gradient estimator (Bengio et al., 2013) for backpropagation optimization (Sec. 2). The learned binary mask indicates positions of certain parameters, which are selected to be masked out. Interestingly, we find removing these weights leads to further performance gain. Fig. 2 shows its details: we start our MFT (red line) from the best FFT model (yellow star), which is a well-trained model and always seen as an upper bound of LLM fine-tuning. The FFT (blue line) performs over-fitting after sufficient training, however, our MFT achieves further improvement. These teaser cases show a consistent observation across different backbones (LLaMA2-7B (Touvron et al., 2023) and LLaMA3.1-8B (Dubey et al., 2024)) and domains (GSM8K (Cobbe et al., 2021), HumanEval (Chen et al., 2021), and IF-Eval (Zhou et al., 2023a) for math, coding, and instruction, respectively). Comparisons of more configurations are elaborated in Sec. 3. Such phenomenon substantially answers the question we are interested in: *the LLM structural integrity is not indispensable for good model performance and breaking such integrity can bring further improvements.*

MFT is a post fine-tuning strategy with further improvement, particularly starting from yet outperforming the FFT upper bound. It is compatible to other existing fine-tuning methods and can be integrated into any of them flexibly. Therefore, it naturally upgrades current fine-tuning routine as a new protocol shown in Fig. 1, providing a new perspective to investigate LLM fine-tuning.

Besides, we emphasize the difference between typical pruning methods and our work. The former one compresses model and tries to maintain the trained model capacity, but the later one aims for further improvement above a well-trained model without compression purpose. Even if they share the same concept of *mask*, their fundamental goals are different (see more discussions in Sec. 4). Furthermore, our study extends the function of mask learning from typical network compression into a more general scenario. In other words, analogically speaking, *typical mask learning employ subtraction to reduce (pruning to compress), whereas our approach leverages subtraction to achieve augmentation (removing weights to improve).*

We summarize this study as below:

- We are curious if the LLM structural integrity is indispensable to good performance and firstly explore if a well-trained LLM can be further improved by removing certain weights to break such structural integrity.
- A mask fine-tuning (MFT) is proposed to substantially

answers our question. It outperforms the FFT upper bound, compatibly upgrading typical LLM fine-tuning protocol, and extends the mask learning functionality from typical network pruning to a general scenario.

- Extensive experiments across different backbones, domains, and FFT settings consistently support our conclusion. Detailed ablation and analysis are provided for a better intuition to inspire more future works.

2. Mask Fine-Tuning

We focus on GPT-like language models (Brown et al., 2020; Radford et al., 2019) in auto-regressive fashion and start from a fully fine-tuned model of a pre-trained language backbone to conduct our mask fine-tuning (MFT). Therefore, we briefly go through language model notations of full fine-tuning (FFT), then introduce our MFT.

Full Fine-Tuning. We refer a pre-trained auto-regressive language backbone as \mathcal{N}_p with parameters Θ_p and optimize the following objective to represent a FFT:

$$L(U_f) = \sum_i \log P(u_f^i | u_f^{i-k}, \dots, u_f^{i-1}; \Theta_p), \quad (1)$$

where L represents the auto-regressive loss to supervise the next token prediction. Θ_p is fully optimized and $U_f = \{u_f^1, \dots, u_f^n\}$ is a token sequence of a language corpus, serving as a FFT dataset. We refer the model after sufficient FFT as \mathcal{N}_f with optimized parameters Θ_f .

Mask Fine-Tuning. We deploy our MFT on model after FFT. Formally, we revise Eq. 1 by adding a binary mask onto model parameters and obtain the rewritten loss for MFT as below:

$$L(U_m) = \sum_i \log P(u_m^i | u_m^{i-k}, \dots, u_m^{i-1}; \Theta_f \odot M). \quad (2)$$

MFT shares the same objective function L as FFT with a different dataset U_m for supervision. The main difference is we add a binary mask M on Θ_f , where they share the same size and corresponding weights are masked out by element-wise multiplication \odot . During MFT, Θ_f is fixed and M is updated. In this way, MFT learns to find locations of certain weights while keeping the fully fine-tuned parameters Θ_f fixed. And these weights can be removed from the well-trained model by applying this learned binary mask. M is optimized by a learnable process leveraged on the straight-through gradient estimator (Bengio et al., 2013), and we name it as learnable mask.

Learnable Mask. Given a model parameter Θ_f after FFT, we represent it in a layer-wise fashion as $\Theta = \{\theta_l\}, l \in \{1, 2, \dots, L\}$, where we omit the subscribe f for notation simplicity. L represents model layer number. Then, we can

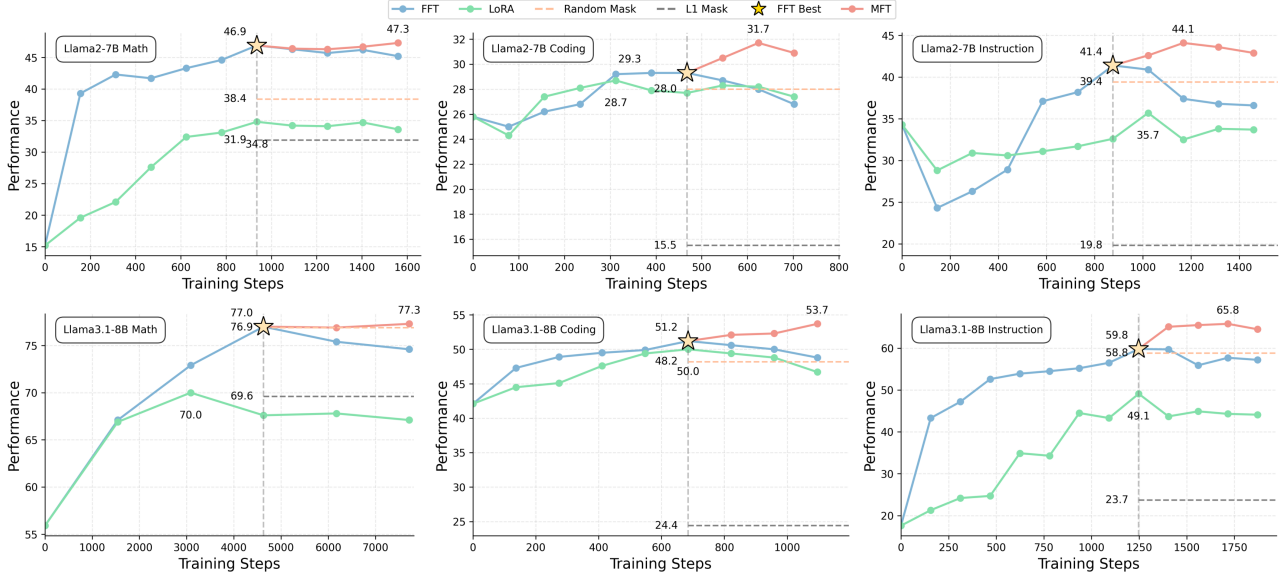


Figure 2. The visualization of performance trend along with different fine-tuning strategies, including FFT (blue line), LoRA (green line) (Hu et al., 2021), and our MFT (red line). We also add random (orange dash) and L1 mask (gray dash) for comparison. We use three settings across LLaMA2 and LLaMA3.1 backbones on GSM8K, HumanEval, and IF-Eval for math, coding, and instruction domains, respectively. The x-axis is training steps starting from the pre-trained backbone. The y-axis is evaluation performance. MFT (red line) starts from the best FFT model (yellow star) and breaks the upper bound with further improvements, while continued FFT leads to over-fitting. It also performs better than LoRA fine-tuning and two vanilla mask baselines.

formalize each layer as

$$I_{l+1} = \sigma(F[I_l; \theta_l]), \quad (3)$$

where I_l is the layer l input and I_{l+1} is its output with activation σ . F generally serves as a layer operation (e.g., convolutional or linear layer) with parameter $\theta_l = \{\theta_l^d\}$, $d \in \{1, 2, \dots, D_l\}$. D_l represents the layer l parameter dimension. In this work, F represents linear layer, as we mainly consider Transformer based language models and deploy mask learning on model linear mappings. To perform mask learning, we fix all parameters Θ denoted as $\bar{\Theta}$. Then, each weight θ_l^d is assigned with a learnable score c_l^d , representing the importance of corresponding weight. Based on this, we rewrite the Eq. 3 as

$$I_{i+1} = \sigma(F[I_i; \bar{\theta}_l \odot v(c_l)]), \quad (4)$$

where $c_l = \{c_l^1, c_l^2, \dots, c_l^{D_l}\}$ is the score of parameter $\bar{\theta}_l$. v is an indicator function to select mask based on scores. In this work, we involve two practices of v for our experiments (Sec. 3): 1) ratio-based one outputs 1 or 0 depending on if the value of c_l^d is in the top $K\%$ highest scores or not. K is a pre-defined mask ratio; 2) threshold-based one outputs 1 when $c_l^d > T$ and outputs 0 otherwise, where T is a pre-defined mask threshold. By updating c with fixed $\bar{\Theta}$, part of parameters in $\bar{\Theta}$ are kept while others are masked out. As the indicator function v is non-derivable, we use the

straight-through gradient estimator (Bengio et al., 2013) to estimate the c_l^d gradient. Concretely, v is regarded as an identity function during gradient backwards step, then the approximation can be described as

$$\tilde{g}(c_l^d) = \frac{\partial L}{\partial \tilde{I}_{l+1}} \frac{\partial \tilde{I}_{l+1}}{\partial c_l^d} \approx \frac{\partial L}{\partial I_{l+1}} \frac{\partial I_{l+1}}{\partial c_l^d}, \quad (5)$$

where $\tilde{I}_{l+1} = \sigma(F[I_l; \bar{\theta}_l \odot c_l])$ after applying estimation and $\tilde{g}(c_l^d)$ is the estimated gradient of score c_l^d . In this way, MFT learns to obtain a mask for model N_f and we denote the final model as N_m with parameter Θ_f and mask M .

MFT is a learnable way to identify certain weights guided by regular training loss of language models, and further remove them by applying the learned mask. It helps to answer our question (Sec. 1) and provide a new LLM fine-tuning protocol. We illustrate the MFT procedure in Fig. 1. Please note, the FFT method used in this study is supervised fine-tuning (SFT) without considering other policy based tuning like DPO (Direct Preference Optimization) (Rafailov et al., 2024) and PPO (Proximal Policy Optimization) (Schulman et al., 2017). Our MFT can be easily generalized onto them but it is out of scope of this work.

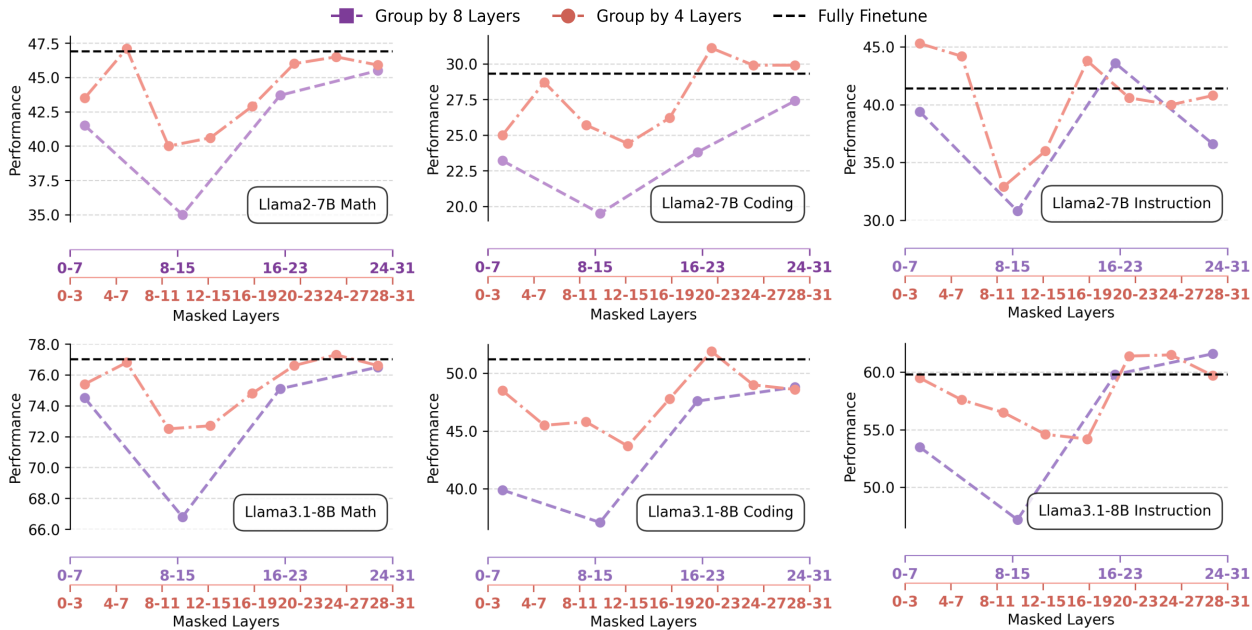


Figure 3. We visualize the ablation study of local MFT strategy. It uses LLaMA2-7B and LLaMA3.1-8B backbones, covering math, coding, and instruction domains. In each figure, we conduct MFT ablations with 10% masking ratio on a domain-specific FFT model (black dash line). We swap the ablation under two local granularities, 8-layer (purple) and 4-layer (orange), from shallow to deep layers with 10% fine-tuning set. We find 1) MFT can outperform the FFT strong baseline and 2) MFT performs better in shallow (0-7) and relatively deep layers (20-27). Please note, this ablation is only for quick intuitions with limited performance gain of MFT using 10% subset. Based on this trend, we deploy MFT with complete fine-tuning sets, achieving more improvements (Tab. 3.1 and Tab. 3.2).

3. Experiments

We evaluate our proposed mask fine-tuning (MFT) on large language models (LLMs) across several backbones, domains, and full fine-tuning (FFT) settings. In addition, we provide ablations and visualization analysis of different aspects to provide a better intuition.

3.1. Preliminaries

Pretrained Backbones. We use Transformer (Vaswani, 2017) based pretrained LLMs as backbone models including LLaMA2-7B (Touvron et al., 2023) and LLaMA3.1-8B (Dubey et al., 2024).

Domains & Datasets. We involve three domains with their representative tasks. Specifically, we include GSM8K (Cobbe et al., 2021) and MetaMath (Yu et al., 2023) for math, HumanEval and HumanEval+ (Chen et al., 2021) for coding, and IF-Eval (Zhou et al., 2023a) and Alpaca-Eval (Dubois et al., 2024) for instruction following domains, respectively. All of these three domains are used for typical FFT, our MFT, and evaluation.

Experimental Configurations. Based on pretrained backbones, our experiments contain FFT, MFT, and downstream evaluation in order. For FFT, we follow two strategies: 1)

domain-specific, 2) mix-up, where the former one conducts FFT using datasets from individual domain from math, coding, or instruction following and the later one using a mix-up datasets from all these domains. For MFT, we follow domain-specific fashion, using datasets from one individual domain. More dataset details are provided in Sec. A.1. We mainly use local masking, which is elaborated by a series proof-of-concept studies in Sec. 3.2 and Fig. 3. We also provide an initial exploration of global masking strategy in Sec. 3.3 and Tab. 3. For evaluation, we comprehensively test performance changes within (Tab. 3.1 and Tab. 3.2) and across domains (Tab. A.2 and Tab. A.2).

Baselines. We use several baselines for comparisons including (1) pre-trained backbone as a very basic baseline; (2) FFT as a strong baseline which is often seen as an upper bound for downstream fine-tuning. We perform sufficient FFT and report the best performance; (3) LoRA (Hu et al., 2021) fine-tuning as a strong alternative of FFT; (4) continued FFT to see if continue training results in further improvement; (5) random mask and (6) L1 mask as two vanilla masking strategies. Among them, (2) FFT and (4) continued FFT are critical to our experiments, since our goal is using MFT to break the limit of FFT upper bound and continued FFT serves as a sanity check of this upper bound.

Method		Math		Coding		Instruction Following	
		GSM8K	Math	HumanEval	HumanEval+	IF-Eval	Alpaca-Eval
Pre-Trained Model (Lower Bound)		15.2	2.5	25.8	22.4	34.3	0.5
Specific Domain	LoRA	34.8	4.7	28.7	23.8	35.7	1.2
	Continued LoRA	33.6	4.5	28.2	23.2	32.5	1.1
	FFT (Upper Bound)	46.9	6.7	29.3	25.0	41.4	1.7
	Continued FFT	45.2 ↓ 1.7	5.7 ↓ 1.0	28.0 ↓ 1.3	23.8 ↓ 1.2	37.4 ↓ 7.0	2.0 ↑ 0.3
	Random Mask w/ Upper Bound	38.4	4.9	28.0	25.0	39.4	1.4
	L1 Mask w/ Upper Bound	31.9	1.0	15.5	14.3	19.8	0.0
	MFT w/ Upper Bound (Ours)	47.3 ↑ 0.4	7.6 ↑ 0.9	31.7 ↑ 2.4	28.0 ↑ 3.0	44.1 ↑ 2.7	2.9 ↑ 1.2
Mixed Domain	LoRA	40.8	6.1	22.6	18.3	37.3	0.7
	Continued LoRA	31.9	4.0	20.1	17.1	18.5	0.8
	FFT (Upper Bound)	45.7	8.2	29.9	26.9	43.8	1.1
	Continued FFT	44.3 ↓ 1.4	7.6 ↓ 0.6	21.3 ↓ 8.6	18.3 ↓ 8.6	38.8 ↓ 5.0	1.3 ↑ 0.2
	Random Mask w/ Upper Bound	40.0	6.5	20.7	17.1	20.0	1.2
	L1 Mask w/ Upper Bound	0.9	0.0	39.6	36.6	33.9	0.1
	MFT w/ Upper Bound (Ours)	45.8 ↑ 0.1	8.3 ↑ 0.1	31.7 ↑ 1.8	27.5 ↑ 0.6	46.3 ↑ 2.5	2.0 ↑ 0.9

Table 1. Performance comparison on LLaMA2-7B of domain-specific (upper part) and multi-domain mix-up FFT settings (lower part). Each part has three blocks containing 1) common LoRA and its continued variant (green), 2) FFT serving as upper bound and its continued variant (blue), and 3) our MFT (red) with other two vanilla masking baselines. The pre-trained model performance is shown on the top, serving as lower bound in our evaluation.

3.2. Main Results

We describe our exploration logic for MFT empirical validation and draw conclusions. As mentioned in Sec. 3.1, our MFT mainly uses local masking strategy, therefore, we start from a proof-of-concept ablation study to test the model component sensitivity to MFT (Fig. 3). Such ablation helps us detect the most effective components of the well-trained model to employ MFT. Accordingly, we extensively deploy MFT in this local fashion across different configurations and compare with strong fine-tuning baselines.

Local Mask Fine-Tuning Ablation. This series of ablations aim to check if the MFT has potential to improve model capacity after FFT. If so, we expect a comprehensive ablation also detects the sensitivity of different model components to MFT strategy. Concretely, we start from LLaMA2-7B and LLaMA3.1-8B backbones after domain-specific FFT and conduct MFT using a small subset of each individual domain. Specifically, for each domain, we use 10% of its corresponding fine-tuning set and details are provided in Sec. A.1. To swap the model, we set continuous 4 or 8 layers as a group to ablate the model from shallow to deep layers. For each given group, we use MFT to locally learn a mask and keep other layers fixed to check model performances. For example, for the layer 4 to 7, it is formally achieved by setting $\Theta = \{\theta_l\}, l \in \{4, 5, 6, 7\}$. Within each target layer group, we use the ratio-based fashion for mask learning and set the masking ratio as 10%, which means we aim to learn and remove 10% parameters while keeping the rest 90%.

Fig. 3 shows the detailed ablation results. We find that 1) compared with FFT, the MFT has potential to make further improvement on each individual configuration (above the black dash line), even if they may not share exactly the same layer-wise location; 2) smaller layer-wise group (4-layer) is better for MFT compared with larger one (8-layer), however, they generally share the similar trend, where shallow (0-7) and mid-to-rear (20-27) partitions response positively to MFT than other parts. Such observation first confirms the MFT potential to further improve fully fine-tuned models, and then indicate promising partitions to conduct mask learning. Concretely, for LLaMA2-7B, we use 4-7, 20-23, and 0-3 for math, coding, and instruction domains, respectively, to conduct our MFT. For LLaMA3.1-8B, we use 24-27, 20-23, and 24-27 for these three domains accordingly.

Please note that (1) since this ablation is only for quick intuition and sanity check of MFT effectiveness, we only use 10% subset here. According to such insights, MFT is trained using complete fine-tuning datasets for more performance gain; (2) since larger layer groups (e.g., 16) achieve significant performance drop, we omit their results in Fig. 3 for a better illustration and supplement them in Sec. A.3.

Comparisons. Tab. 3.1 and Tab. 3.2 show our main comparisons on LLaMA2-7B and LLaMA3.1-8B backbones. We start from a pre-trained model (lower bound) followed by two FFT settings using fine-tuning dataset of specific and mixed domains for each backbone. For each setting, we use FFT serving as upper bound and its continued version

Boosting Large Language Models with Mask Fine-Tuning

Method		Math		Coding		Instruction Following	
		GSM8K	Math	HumanEval	HumanEval+	IF-Eval	Alpaca-Eval
Pre-Trained Model (Lower Bound)		55.9	14.6	42.1	37.8	17.6	9.0
Specific Domain	LoRA	70.0	22.7	50.0	45.1	49.1	10.1
	Continued LoRA	67.1	19.7	46.7	44.5	44.3	8.9
	FFT (Upper Bound)	77.0	24.3	51.2	45.1	59.8	12.0
	Continued FFT	74.6 ↓ _{2.4}	24.0 ↓ _{0.3}	48.8 ↓ _{2.4}	42.1 ↓ _{3.0}	57.7 ↓ _{2.1}	11.4 ↓ _{0.6}
	Random Mask w/ Upper Bound	76.9	22.3	48.2	42.7	58.8	11.5
	L1 Mask w/ Upper Bound	69.6	16.2	24.4	20.7	23.7	0.6
	MFT w/ Upper Bound (Ours)	77.3 ↑ _{0.3}	24.9 ↑ _{0.6}	53.7 ↑ _{2.5}	47.0 ↑ _{1.9}	65.8 ↑ _{6.0}	13.8 ↑ _{1.8}
Multi Domain	LoRA	72.8	24.1	59.1	55.5	38.2	11.0
	Continued LoRA	70.4	24.5	63.1	55.3	32.1	5.3
	FFT (Upper Bound)	72.9	24.5	64.6	60.4	60.2	11.9
	Continued FFT	71.9 ↓ _{1.0}	24.3 ↓ _{2.2}	62.8 ↓ _{1.8}	58.5 ↓ _{1.9}	59.9 ↓ _{0.3}	8.9 ↓ _{2.0}
	Random Mask w/ Upper Bound	72.6	23.3	59.1	55.5	56.8	7.0
	L1 Mask w/ Upper Bound	62.7	15.3	39.6	36.6	44.0	0.7
	MFT w/ Upper Bound (Ours)	73.8 ↑ _{0.9}	25.3 ↑ _{0.8}	66.5 ↑ _{1.9}	61.6 ↑ _{1.2}	62.5 ↑ _{2.3}	12.3 ↑ _{0.4}

Table 2. Performance comparison on LLaMA3.1-8B of domain-specific (upper part) and multi-domain mix-up FFT settings (lower part). Each part has three blocks containing 1) common LoRA and its continued variant (green), 2) FFT serving as upper bound and its continued variant (blue), and 3) our MFT (red) with other two vanilla masking baselines. The pre-trained model performance is shown on the top, serving as lower bound in our evaluation.

Method	LLaMA2-7B		LLaMA3.1-8B	
	GSM8K	Math	GSM8K	Math
Pre-Trained Model	15.2	2.5	55.9	14.6
FFT	46.9	6.7	77.0	24.3
Continued FFT	45.2 ↓ _{1.7}	5.7 ↓ _{1.0}	74.6 ↓ _{2.4}	24.0 ↓ _{0.3}
FFT + Global MFT (Ours)	49.0 ↑ _{2.1}	7.1 ↑ _{0.4}	74.1 ↓ _{2.9}	21.8 ↓ _{2.5}

Table 3. Initial exploration of global MFT on math domain using LLaMA2-7B and LLaMA3.1-8B backbones. We observe better performance on LLaMA2-7B, especially for GSM8K, but performance drop on LLaMA3.1-8B.

(blue) with LoRA and its continued variant as alternative baselines (green). We also include random and L1 mask as two vanilla masking baselines (white). Our MFT (red) is starting from the FFT (upper bound) and further improves the model capacity. Among them, two critical baselines are FFT and continued FFT, where the former one serves as the upper bound performance and the later one as a sanity check of this upper bound and also indicating the potential performance drop due to overfitting issue. We train our MFT only using domain specific datasets for both two FFT scenarios. Tab. 3.1 and Tab. 3.2 only show the evaluation within the MFT fine-tuning domain, and we supplement the cross domain evaluation in Tab. A.2 and Tab. A.2 of Sec. A.2. Accordingly, we draw conclusions: 1) Since the continued FFT causes performance drop due to over-fitting for all settings (red downward arrow), the FFT upper bound passes the sanity check. In addition, such upper bound outperforms other comparison methods, thus, it is reason-

able to set it as our strong baseline to start with, supporting us to draw following conclusions. 2) Our MFT achieves promising and consistent improvements across different backbones, domains, and FFT configurations (green upward arrow). Since MFT outperforms FFT upper bound, such performance gain indicates fundamental improvement of LLM fine-tuning. It accordingly upgrades current routine as a new LLM fine-tuning protocol by learning and applying a mask on a well-trained model. Besides, other two masking baselines generally damage the performance, indicating such mask learning process is not a trivial step and valuable to explore, especially compared with consistent improvement given by MFT.

3.3. Analyses

We provide further analyses from several perspectives: (1) global MFT exploration, (2) masking ratio ablation, and (3) MFT data ratio ablation.

Global Masking Fine-Tuning. Instead of making ablation to test layer-wise sensitivity then comprehensively deploying local MFT introduced above, we provide a initial exploration for MFT in a global way. Different from local one using ratio based selection, global alternative uses threshold based way. As an initial exploration, we expect it encourages the MFT to automatically detect the appropriate sparse ratio. Specifically, we use math domain on LLaMA2-7B and LLaMA3.1-8B for the global MFT. And we set the threshold as -0.035. Tab. 3 shows the evaluation on math

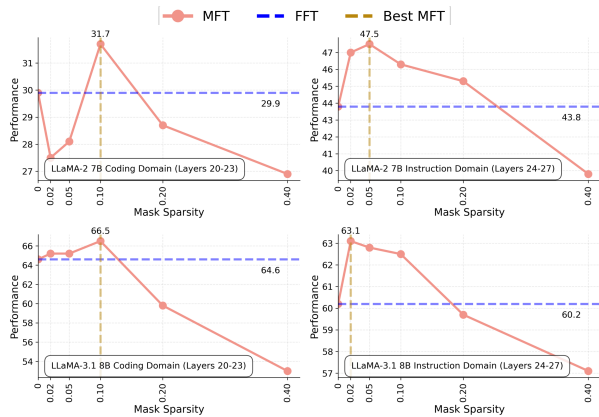


Figure 4. Masking ratio ablation visualizations. We use coding and instruction domains on LLaMA2 and LLaMA3.1 backbones. We observe the original 10% ratio works well on coding but not the optimal one on instruction, which indicates the masking ratio matters and more improvement potential for MFT strategy.

domain. We find that global mask performs better than local one using LLaMA2 on GSM8K, but causes performance drop using LLaMA3.1-8B. Such results indicate the global mask has more potential for further improvement, but may require more systematical investigation, and we leave it to our future work.

Masking Ratio Ablation. We ablate masking ratio for local MFT. In Tab. 3.1 and Tab. 3.2, we consider 10% for masking ratio for all settings, which is a manually set but may not be an optimal option. In this section, we set a series of masking ratios to test its function to the final performance. Specifically, we use all three domains on two backbones and set masking ratio from 0.02 to 0.4. Results of coding and instruction are shown in Fig. 3.3 and we leave math results in Fig. 8 due to the limited space. We find our original ratio 10% works well on certain coding cases. However, it is not optimal for instruction domain, where smaller ratio works better than 10%. Such observation indicates the masking ratio of MFT does matter to the final performances. In addition, it is also valuable to explore if we set different masking ratio on different layers and types of linear mappings (projections in attention and MLP blocks). Such exploration also naturally fit global design to study if more fine-grained masking strategy makes further improvement.

Data Ratio Ablation. We ablate data by different ratios for MFT by keeping other training configurations. Fig. 3.3 shows the performance trends of math and instruction following domains on LLaMA2-7B and LLaMA3.1-8B backbones. We find MFT (purple) with full dataset always leads to model improvement compared with FFT upper bound (red dash line), however, less data may also obtain competitive results in a much more efficient way. Visualization of code domain is supplemented in Fig 9.

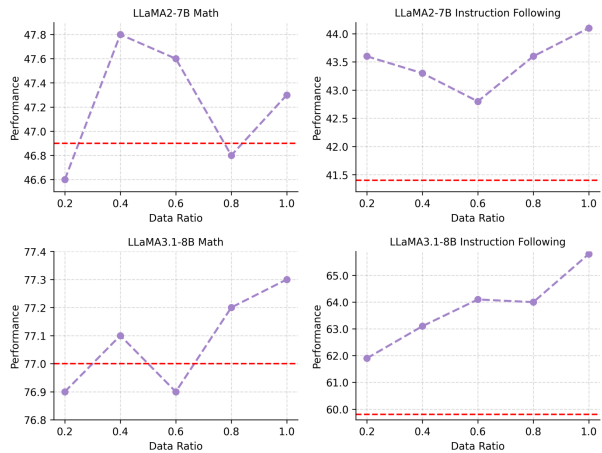


Figure 5. Data ratio ablation visualizations. We use math and instruction domains on LLaMA2 and LLaMA3.1 backbones. Compared with FFT upper bound (red dash line), we observe MFT (purple) always improves the model using full dataset, but it may still obtain promising performance gain using less data.

3.4. Mask Fine-Tuning Loss Landscape

Loss surface visualization is commonly used to analyze the model optimization process, sharing the insight of model status from loss perspective, therefore, we visualize the loss surface of MFT to illustrate its training dynamics. Fig. 6 shows the surface of LLaMA2-7B on math and instruction following domains. The FFT upper bound, continued FFT, and MFT are represented by green star, purple rectangle, and red triangle, respectively. We find MFT always optimizes the model to a better status compared with FFT start point and its continued version resulting in over-fitting for both training and test. We supplement loss surface for coding domain in Fig 10.

4. Related Work

This work explores to optimize a well-trained large language model (LLM) by learning a binary mask and proposes the mask fine-tuning (MFT), upgrading current LLM fine-tuning protocol. We summarize relevant literature of our work from (1) LLM pre-training and fine-tuning and (2) sparse network perspectives, emphasizing their correlations and differences.

4.1. Large Language Models Pre-training & Fine-tuning

LLM pre-training leads to significant performance gain for general language model capacity for both understanding (Devlin, 2018; Raffel et al., 2020; Liu, 2019; He et al., 2020) and generation (Radford et al., 2019; Brown et al., 2020; Achiam et al., 2023; Dubey et al., 2024; Touvron et al., 2023). Massive language corpus with large-scale pre-

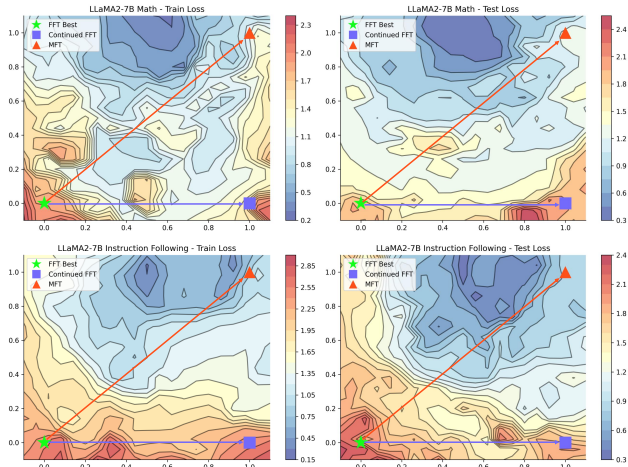


Figure 6. The loss landscape visualization on math and instruction following domains using LLaMA2-7B. Such visualization indicates the proposed MFT further refines the upper bound model to a better optimization and generalization status.

training enable them being strong language backbones with basic common knowledge. Following pre-training, downstream fine-tuning based on small but high quality target datasets further enhance pre-trained models with specific capacities of target domains (Hendrycks et al., 2021; Yu et al., 2023; Cobbe et al., 2021; Chen et al., 2021; Austin et al., 2021; Zhou et al., 2023a; Wang et al., 2023; Nguyen, 2023). Different fine-tuning optimization strategies deliver various LLM properties such as supervised fine-tuning (SFT) follows pre-training objective to involve extra domain knowledge into LLM (Taori et al., 2023; Chiang et al., 2023; Wang et al., 2022) and policy based fine-tuning methods better align the human preference with LLM (Schulman et al., 2017; Rafailov et al., 2024; Ivison et al., 2024; Ouyang et al., 2022; Dai et al., 2023). We propose a mask fine-tuning (MFT) as a post fine-tuning strategy to further refine fine-tuned LLM, especially for SFT in this study. Such strategy can be flexibly deployed after any fine-tuned model to propose a new protocol to improve LLMs.

4.2. Sparse Networks

Model sparsity in neural networks is close to neural network pruning (Liu et al., 2018; Molchanov et al., 2016; Wang et al., 2021) for model compression (Han et al., 2015; Iandola, 2016) and acceleration (Han et al., 2016; Wang et al., 2020; Wang & Fu, 2022; Ma et al., 2023; Fang et al., 2023). Our work shares some overlaps with network pruning, since both aim to find a model partition with certain sparsity, however, pruning tries to remove a large part of model for efficiency while ours focuses on remove parameters irrelevant even harmful to model capacities, which may only take a small model partition. More importantly, pruning methods are always accompanied with performance loss of the

trained model, while ours targets on its further enhancement. In addition, the sparsity concept is also involved into other machine learning fields such as network optimization (Srivastava et al., 2014; Srinivas et al., 2017; Baldi & Sadowski, 2013), model architecture design (Shazeer et al., 2017; Zoph, 2016; Elsken et al., 2019), lottery ticket hypothesis (Frankle & Carbin, 2018; Zhou et al., 2019; You et al., 2019; Bai et al., 2022b), neural network mechanism (Wortsman et al., 2020; Ramanujan et al., 2020; Bai et al., 2022a), etc. In our study, we introduce the sparsity concept to explore if all parameters are beneficial for a well-trained LLM and further improve the model by learning and applying a mask on it, proposing a new way for LLM fine-tuning.

5. Discussion and Conclusion

Intuition. Our propose mask fine-tuning (MFT) is highly relevant to a series well-established research topics like sparse network training, network pruning, model compression, etc. However, inspired by their techniques, we extend the model sparsity function from a efficiency aspect to a more general one, removing negative components for further improvements. In other words, sparse models typical aim to compress model while maintaining performance (seen as *subtraction*, however, our study uses sparsity as a tool for model enhancement (seen as *addition*). We expect such counter-thinking of sparse network inspires more general explorations in the future to enrich its research potentials.

Limitation. Due to vast number of the pre-trained models, domains, and evaluation benchmarks in the community, this work only considers representative ones to delivery a complete exploration pipeline. In addition, we only involve pure language models in this work, and extending it into multi-modal area will further support our statement and conclusion. Through our exploration, we observe interesting phenomena including the sensitivity trend of MFT (Fig. 3), MFT showing promising results with very limited optimization steps (Fig. 2), initial try of global MFT not consistently working well (Fig. 3), etc. Detailed investigation of these points potentially further strengthens the MFT.

Conclusion. We challenge the necessity of large language models (LLMs) structural integrity to study if a well-trained LLM can be further improved by removing certain model parameters. We propose a mask fine-tuning (MFT) to explore it based on model with sufficient full fine-tuning (FFT). MFT positively proves MFT effectiveness, generally improves LLM capacity, and naturally upgrades LLM fine-tuning pipeline. Comprehensive experiments with detailed ablations support our conclusion with exploration intuitions, covering different pre-trained LLM backbones, downstream domains, and fine-tuning configurations. Meanwhile, MFT also extends the functionality of sparse network for a general learning purpose to inspire more future works.

Impact Statement

This paper aims to propose a new LLM fine-tuning protocol based on the proposed MFT strategy. It potentially benefits all LLM fine-tuning strategy. The datasets used for training and evaluation are all open public ones without involving any private resources. Therefore, there is no potential negative social impact of this paper, based on our best knowledge.

References

- Achiam, J., Adler, S., Agarwal, S., Ahmad, L., Akkaya, I., Aleman, F. L., Almeida, D., Altenschmidt, J., Altman, S., Anadkat, S., et al. Gpt-4 technical report. *arXiv preprint arXiv:2303.08774*, 2023.
- Austin, J., Odena, A., Nye, M., Bosma, M., Michalewski, H., Dohan, D., Jiang, E., Cai, C., Terry, M., Le, Q., et al. Program synthesis with large language models. *arXiv preprint arXiv:2108.07732*, 2021.
- Bai, Y., Wang, H., Ma, X., Zhang, Y., Tao, Z., and Fu, Y. Parameter-efficient masking networks. *NeurIPS*, 2022a.
- Bai, Y., Wang, H., Tao, Z., Li, K., and Fu, Y. Dual lottery ticket hypothesis. *arXiv preprint arXiv:2203.04248*, 2022b.
- Baldi, P. and Sadowski, P. J. Understanding dropout. *NeurIPS*, 2013.
- Bengio, Y., Léonard, N., and Courville, A. Estimating or propagating gradients through stochastic neurons for conditional computation. *arXiv preprint arXiv:1308.3432*, 2013.
- Brown, T., Mann, B., Ryder, N., Subbiah, M., Kaplan, J. D., Dhariwal, P., Neelakantan, A., Shyam, P., Sastry, G., Askell, A., et al. Language models are few-shot learners. *NeurIPS*, 2020.
- Chaudhary, S. Code alpaca: An instruction-following llama model for code generation, 2023.
- Chen, M., Tworek, J., Jun, H., Yuan, Q., Pinto, H. P. D. O., Kaplan, J., Edwards, H., Burda, Y., Joseph, N., Brockman, G., et al. Evaluating large language models trained on code. *arXiv preprint arXiv:2107.03374*, 2021.
- Chiang, W.-L., Li, Z., Lin, Z., Sheng, Y., Wu, Z., Zhang, H., Zheng, L., Zhuang, S., Zhuang, Y., Gonzalez, J. E., et al. Vicuna: An open-source chatbot impressing gpt-4 with 90%* chatgpt quality. <https://vicuna.lmsys.org>, 2023.
- Cobbe, K., Kosaraju, V., Bavarian, M., Chen, M., Jun, H., Kaiser, L., Plappert, M., Tworek, J., Hilton, J., Nakano, R., et al. Training verifiers to solve math word problems. *arXiv preprint arXiv:2110.14168*, 2021.
- Dai, J., Pan, X., Sun, R., Ji, J., Xu, X., Liu, M., Wang, Y., and Yang, Y. Safe rlhf: Safe reinforcement learning from human feedback. *arXiv preprint arXiv:2310.12773*, 2023.
- Devlin, J. Bert: Pre-training of deep bidirectional transformers for language understanding. *arXiv preprint arXiv:1810.04805*, 2018.
- Dubey, A., Jauhri, A., Pandey, A., Kadian, A., Al-Dahle, A., Letman, A., Mathur, A., Schelten, A., Yang, A., Fan, A., et al. The llama 3 herd of models. *arXiv preprint arXiv:2407.21783*, 2024.
- Dubois, Y., Galambosi, B., Liang, P., and Hashimoto, T. B. Length-controlled alpacaEval: A simple way to debias automatic evaluators. *arXiv preprint arXiv:2404.04475*, 2024.
- Elsken, T., Metzger, J. H., and Hutter, F. Neural architecture search: A survey. *JMLR*, 2019.
- Fang, G., Ma, X., and Wang, X. Structural pruning for diffusion models. In *NeurIPS*, 2023.
- Frankle, J. and Carbin, M. The lottery ticket hypothesis: Finding sparse, trainable neural networks. *arXiv preprint arXiv:1803.03635*, 2018.
- Frieder, S., Pinchetti, L., Griffiths, R.-R., Salvatori, T., Lukasiewicz, T., Petersen, P., and Berner, J. Mathematical capabilities of chatgpt. *NeurIPS*, 2024.
- Han, S., Mao, H., and Dally, W. J. Deep compression: Compressing deep neural networks with pruning, trained quantization and Huffman coding. *arXiv preprint arXiv:1510.00149*, 2015.
- Han, S., Liu, X., Mao, H., Pu, J., Pedram, A., Horowitz, M. A., and Dally, W. J. Eie: Efficient inference engine on compressed deep neural network. *ACM SIGARCH Computer Architecture News*, 2016.
- He, P., Liu, X., Gao, J., and Chen, W. Deberta: Decoding-enhanced bert with disentangled attention. *arXiv preprint arXiv:2006.03654*, 2020.
- Hendrycks, D., Burns, C., Kadavath, S., Arora, A., Basart, S., Tang, E., Song, D., and Steinhardt, J. Measuring mathematical problem solving with the math dataset. *arXiv preprint arXiv:2103.03874*, 2021.
- Houlsby, N., Giurgiu, A., Jastrzebski, S., Morrone, B., De Laroussilhe, Q., Gesmundo, A., Attariyan, M., and Gelly, S. Parameter-efficient transfer learning for nlp. In *ICML*, 2019.

- Hu, E. J., Shen, Y., Wallis, P., Allen-Zhu, Z., Li, Y., Wang, S., Wang, L., and Chen, W. Lora: Low-rank adaptation of large language models. *arXiv preprint arXiv:2106.09685*, 2021.
- Iandola, F. N. Squeezenet: Alexnet-level accuracy with 50x fewer parameters and 0.5 mb model size. *arXiv preprint arXiv:1602.07360*, 2016.
- Iverson, H., Wang, Y., Liu, J., Wu, Z., Pyatkin, V., Lambert, N., Smith, N. A., Choi, Y., and Hajishirzi, H. Unpacking dpo and ppo: Disentangling best practices for learning from preference feedback. *arXiv preprint arXiv:2406.09279*, 2024.
- Köpf, A., Kilcher, Y., von Rütte, D., Anagnostidis, S., Tam, Z.-R., Stevens, K., Barhoum, A., Duc, N. M., Stanley, O., Nagyfi, R., ES, S., Suri, S., Glushkov, D., Dantuluri, A., Maguire, A., Schuhmann, C., Nguyen, H., and Mattick, A. Openassistant conversations – democratizing large language model alignment, 2023. URL <https://arxiv.org/abs/2304.07327>.
- Lambert, N., Morrison, J., Pyatkin, V., Huang, S., Iverson, H., Brahman, F., Miranda, L. J. V., Liu, A., Dziri, N., Lyu, S., Gu, Y., Malik, S., Graf, V., Hwang, J. D., Yang, J., Bras, R. L., Taffjord, O., Wilhelm, C., Soldaini, L., Smith, N. A., Wang, Y., Dasigi, P., and Hajishirzi, H. Tulu 3: Pushing frontiers in open language model post-training, 2025. URL <https://arxiv.org/abs/2411.15124>.
- Lewkowycz, A., Andreassen, A., Dohan, D., Dyer, E., Michalewski, H., Ramasesh, V., Slone, A., Anil, C., Schlag, I., Gutman-Solo, T., Wu, Y., Neysshabur, B., Gur-Ari, G., and Misra, V. Solving quantitative reasoning problems with language models, 2022.
- LI, J., Beeching, E., Tunstall, L., Lipkin, B., Soletskyi, R., Huang, S. C., Rasul, K., Yu, L., Jiang, A., Shen, Z., Qin, Z., Dong, B., Zhou, L., Fleureau, Y., Lample, G., and Polu, S. Numinamath tir, 2024.
- Li, X., Zhang, T., Dubois, Y., Taori, R., Gulrajani, I., Guestrin, C., Liang, P., and Hashimoto, T. B. AlpacaEval: An automatic evaluator of instruction-following models, 2023.
- Liu, J., Xia, C. S., Wang, Y., and Zhang, L. Is your code generated by chatGPT really correct? rigorous evaluation of large language models for code generation. In *NeurIPS*, 2023.
- Liu, Y. Roberta: A robustly optimized bert pretraining approach. *arXiv preprint arXiv:1907.11692*, 2019.
- Liu, Z., Sun, M., Zhou, T., Huang, G., and Darrell, T. Rethinking the value of network pruning. *arXiv preprint arXiv:1810.05270*, 2018.
- Luo, Z., Xu, C., Zhao, P., Sun, Q., Geng, X., Hu, W., Tao, C., Ma, J., Lin, Q., and Jiang, D. Wizardcoder: Empowering code large language models with evol-instruct, 2023.
- Ma, X., Fang, G., and Wang, X. Llm-pruner: On the structural pruning of large language models. *NeurIPS*, 2023.
- Molchanov, P., Tyree, S., Karras, T., Aila, T., and Kautz, J. Pruning convolutional neural networks for resource efficient inference. *arXiv preprint arXiv:1611.06440*, 2016.
- Mukherjee, S., Mitra, A., Jawahar, G., Agarwal, S., Palangi, H., and Awadallah, A. Orca: Progressive learning from complex explanation traces of gpt-4, 2023. URL <https://arxiv.org/abs/2306.02707>.
- Nguyen, H.-T. A brief report on lawgpt 1.0: A virtual legal assistant based on gpt-3. *arXiv preprint arXiv:2302.05729*, 2023.
- Ouyang, L., Wu, J., Jiang, X., Almeida, D., Wainwright, C., Mishkin, P., Zhang, C., Agarwal, S., Slama, K., Ray, A., et al. Training language models to follow instructions with human feedback. *NeurIPS*, 2022.
- Radford, A., Wu, J., Child, R., Luan, D., Amodei, D., Sutskever, I., et al. Language models are unsupervised multitask learners. *OpenAI Blog*, 2019.
- Rafailov, R., Sharma, A., Mitchell, E., Manning, C. D., Ermon, S., and Finn, C. Direct preference optimization: Your language model is secretly a reward model. *NeurIPS*, 2024.
- Raffel, C., Shazeer, N., Roberts, A., Lee, K., Narang, S., Matena, M., Zhou, Y., Li, W., and Liu, P. J. Exploring the limits of transfer learning with a unified text-to-text transformer. *JMLR*, 2020.
- Ramanujan, V., Wortsman, M., Kembhavi, A., Farhadi, A., and Rastegari, M. What’s hidden in a randomly weighted neural network? In *CVPR*, 2020.
- Schulman, J., Wolski, F., Dhariwal, P., Radford, A., and Klimov, O. Proximal policy optimization algorithms. *arXiv preprint arXiv:1707.06347*, 2017.
- Shazeer, N., Mirhoseini, A., Maziarz, K., Davis, A., Le, Q., Hinton, G., and Dean, J. Outrageously large neural networks: The sparsely-gated mixture-of-experts layer. *arXiv preprint arXiv:1701.06538*, 2017.
- Srinivas, S., Subramanya, A., and Venkatesh Babu, R. Training sparse neural networks. In *CVPR Workshops*, pp. 138–145, 2017.

- Srivastava, N., Hinton, G., Krizhevsky, A., Sutskever, I., and Salakhutdinov, R. Dropout: a simple way to prevent neural networks from overfitting. *JMLR*, 2014.
- Taori, R., Gulrajani, I., Zhang, T., Dubois, Y., Li, X., Guestrin, C., Liang, P., and Hashimoto, T. B. Alpaca: A strong, replicable instruction-following model. *Stanford Center for Research on Foundation Models*, 2023.
- Touvron, H., Martin, L., Stone, K., Albert, P., Almahairi, A., Babaei, Y., Bashlykov, N., Batra, S., Bhargava, P., Bhosale, S., et al. Llama 2: Open foundation and fine-tuned chat models. *arXiv preprint arXiv:2307.09288*, 2023.
- Vaswani, A. Attention is all you need. *NeurIPS*, 2017.
- Wang, G., Yang, G., Du, Z., Fan, L., and Li, X. Clinical-gpt: large language models finetuned with diverse medical data and comprehensive evaluation. *arXiv preprint arXiv:2306.09968*, 2023.
- Wang, H. and Fu, Y. Trainability preserving neural pruning. *arXiv preprint arXiv:2207.12534*, 2022.
- Wang, H., Qin, C., Zhang, Y., and Fu, Y. Neural pruning via growing regularization. *arXiv preprint arXiv:2012.09243*, 2020.
- Wang, H., Qin, C., Bai, Y., Zhang, Y., and Fu, Y. Recent advances on neural network pruning at initialization. *arXiv preprint arXiv:2103.06460*, 2021.
- Wang, Y., Kordi, Y., Mishra, S., Liu, A., Smith, N. A., Khoshdel, D., and Hajishirzi, H. Self-instruct: Aligning language models with self-generated instructions. *arXiv preprint arXiv:2212.10560*, 2022.
- Wortsman, M., Ramanujan, V., Liu, R., Kembhavi, A., Rastegari, M., Yosinski, J., and Farhadi, A. Supermasks in superposition. *NeurIPS*, 2020.
- You, H., Li, C., Xu, P., Fu, Y., Wang, Y., Chen, X., Baraniuk, R. G., Wang, Z., and Lin, Y. Drawing early-bird tickets: Towards more efficient training of deep networks. *arXiv preprint arXiv:1909.11957*, 2019.
- Yu, L., Jiang, W., Shi, H., Yu, J., Liu, Z., Zhang, Y., Kwok, J. T., Li, Z., Weller, A., and Liu, W. Metamath: Bootstrap your own mathematical questions for large language models. *arXiv preprint arXiv:2309.12284*, 2023.
- Zhou, H., Lan, J., Liu, R., and Yosinski, J. Deconstructing lottery tickets: Zeros, signs, and the supermask. *NeurIPS*, 2019.
- Zhou, J., Lu, T., Mishra, S., Brahma, S., Basu, S., Luan, Y., Zhou, D., and Hou, L. Instruction-following evaluation for large language models. *arXiv preprint arXiv:2311.07911*, 2023a.
- Zhou, J., Lu, T., Mishra, S., Brahma, S., Basu, S., Luan, Y., Zhou, D., and Hou, L. Instruction-following evaluation for large language models, 2023b. URL <https://arxiv.org/abs/2311.07911>.
- Zoph, B. Neural architecture search with reinforcement learning. *arXiv preprint arXiv:1611.01578*, 2016.

A. Appendix

A.1. Implementations

We generally conduct our MFT 2 epochs with 8 as batch size on 8*A100 GPUs for different settings. Learning rates are set as $2e-5$ and $5e-6$ for LLaMA2-7B and LLaMA3.1-8B, respectively. We show the datasets details in our experiments for both training and test in Tab.4.

Domain	Train / Test	Dataset Name	# of Samples
Math	Train	Tulu 3 Persona MATH (Lambert et al., 2025)	149,960
		Tulu 3 Persona GSM (Lambert et al., 2025)	49,980
		Tulu 3 Persona Algebra (Lambert et al., 2025)	20,000
		MetaMathQA (Yu et al., 2023)	395,000
		NuminaMath-TIR (LI et al., 2024)	64,312
	Test	GSM8K (Cobbe et al., 2021)	1,320
		MATH (Lewkowycz et al., 2022)	5,003
Coding	Train	Evol CodeAlpaca (Luo et al., 2023)	107,276
		Code-Alpaca (Chaudhary, 2023)	20,022
		Tulu 3 Persona Python (Lambert et al., 2025)	34,999
	Test	HumanEval (Chen et al., 2021)	164
		HumanEval+ (Liu et al., 2023)	164
Instruction Following	Train	OpenAssistant Guanaco (Köpf et al., 2023)	7,132
		Tulu 3 Persona IF (Lambert et al., 2025)	29,980
		Open-Orca (Mukherjee et al., 2023)	30,000
	Test	IFEval (Zhou et al., 2023b)	100
		AlpacaEval 2.0 (Li et al., 2023)	805

Table 4. Dataset information of three domains used in our experiments.

A.2. More Evaluations

Tab. A.2 and Tab. A.2 extend Tab. 3.1 and Tab. 3.2 by adding cross-domain evaluations for our MFT, FFT, and other comparison methods, under domain specific FFT setting.

A.3. More Ablations and Visualizations

We supplement more ablation studies and visualizations: 1) Larger layer-wise group (16-layers) ablation for local MFT shown in Fig. 7, corresponding to Fig. 3. 2) The mask ratio ablation on math domain using LLaMA2-7B and LLaMA3.1-8B shown in Fig.8, corresponding to Fig. 3.3. 3) The MFT data ratio ablation on coding domain using LLaMA2-7B and LLaMA3.1-8B shown in Fig. 9, corresponding to Fig. 3.3. 4) Loss landscape visualization on coding domain using LLaMA2-7B shown in Fig. 10, corresponding to Fig. 6.

Boosting Large Language Models with Mask Fine-Tuning

Method	Math		Coding		Instruction Following	
	GSM8K	Math	HumanEval	HumanEval+	IF-Eval	Alpaca-Eval
[Lower Bound] Base Model	15.2	2.5	25.8	22.4	34.3	0.5
[Upper Bound] FFT [Math]	46.9	6.7	17.7	15.9	29.3	1.5
[Upper Bound] FFT [Coding]	14.6	2.8	29.3	25.0	8.3	1.4
[Upper Bound] FFT [IF]	25.0	2.4	16.5	13.4	41.4	1.7
FFT + Continued FFT [Math]	45.2	5.7	19.5	17.1	33.2	1.5
FFT + Continued FFT [Coding]	11.1	2.5	28.0	23.8	13.1	2.7
FFT + Continued FFT [IF]	23.1	2.1	13.1	12.8	37.4	2.0
Random Mask w/ Upper Bound [Math]	38.4	4.9	14.0	12.8	30.6	1.3
Random Mask w/ Upper Bound [Coding]	14.6	2.5	28.0	25.0	7.3	1.8
Random Mask w/ Upper Bound [IF]	15.1	2.9	12.2	11.6	39.4	1.4
L1 Mask w/ Upper Bound [Math]	31.9	0.0	0.0	0.0	23.9	0.2
L1 Mask w/ Upper Bound [Coding]	7.1	0.3	15.5	4.3	11.8	0.4
L1 Mask w/ Upper Bound [IF]	0.0	0.0	0.0	0.0	19.8	0.0
[Ours] FFT + Mask [Math]	47.3	7.6	16.5	14.6	30.1	0.5
[Ours] FFT + Mask [Coding]	13.8	2.8	31.7	28.0	8.5	2.1
[Ours] FFT + Mask [IF]	23.5	2.8	15.2	11.6	44.1	2.9

Table 5. Extended cross-domain evaluations on LLaMA2-7B under domain specific FFT setting.

Method	Math		Coding		Instruction Following	
	GSM8K	Math	HumanEval	HumanEval+	IF-Eval	Alpaca-Eval
[Lower Bound] Base Model	55.9	14.6	42.1	37.8	17.6	9.0
[Upper Bound] FFT [Math]	77.0	24.3	35.4	29.9	31.5	0.6
[Upper Bound] FFT [Coding]	60.7	13.8	51.2	45.1	5.3	0.9
[Upper Bound] FFT [IF]	63.0	10.1	50.0	44.5	59.8	12.0
FFT + Continued FFT [Math]	74.6	24.0	33.5	31.1	32.2	0.7
FFT + Continued FFT [Coding]	59.6	13.1	48.8	42.1	4.8	1.4
FFT + Continued FFT [IF]	63.6	8.7	45.7	43.5	57.2	11.4
Random Mask w/ Upper Bound [Math]	76.9	22.3	37.8	33.5	30.8	0.5
Random Mask w/ Upper Bound [Coding]	58.9	12.6	48.2	42.7	5.0	1.0
Random Mask w/ Upper Bound [IF]	61.3	6.9	50.0	43.9	58.8	11.5
L1 Mask w/ Upper Bound [Math]	69.6	16.2	29.3	25.0	28.1	0.5
L1 Mask w/ Upper Bound [Coding]	28.3	4.0	24.4	20.7	3.0	0.2
L1 Mask w/ Upper Bound [IF]	44.7	2.6	17.1	14.6	23.7	0.6
[Ours] FFT + Mask [Math]	77.3	24.9	36.0	32.2	31.1	0.5
[Ours] FFT + Mask [Coding]	58.6	13.6	53.7	47.0	4.9	0.0
[Ours] FFT + Mask [Instruction]	63.2	9.6	44.5	40.9	65.8	13.8

Table 6. Extended cross-domain evaluations on LLaMA3.1-8B under domain specific FFT setting.

Boosting Large Language Models with Mask Fine-Tuning

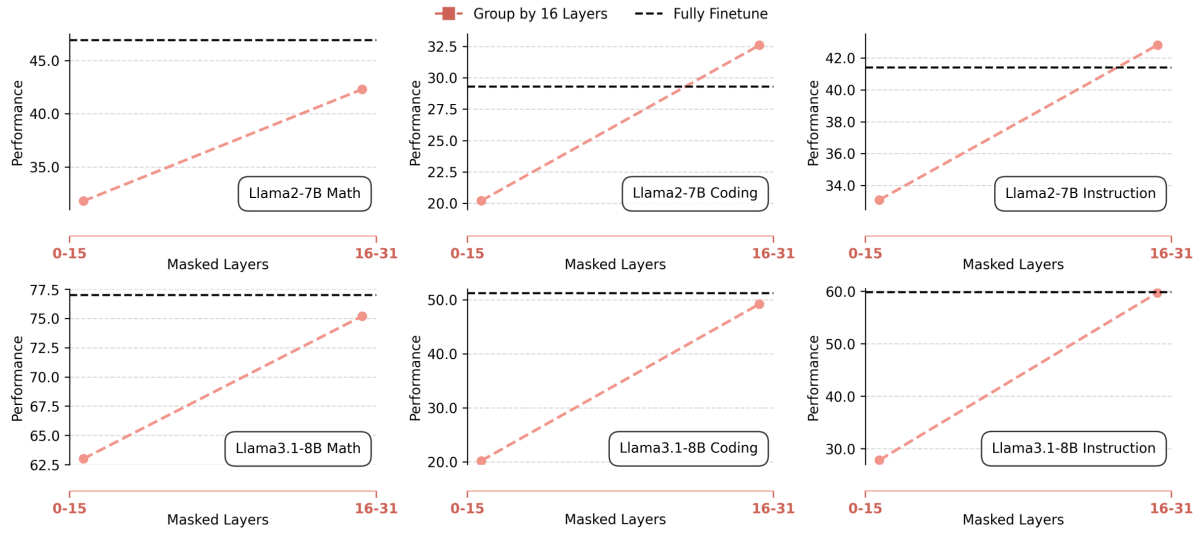


Figure 7. The local MFT ablation results of larger layer-wise group (16-layer).

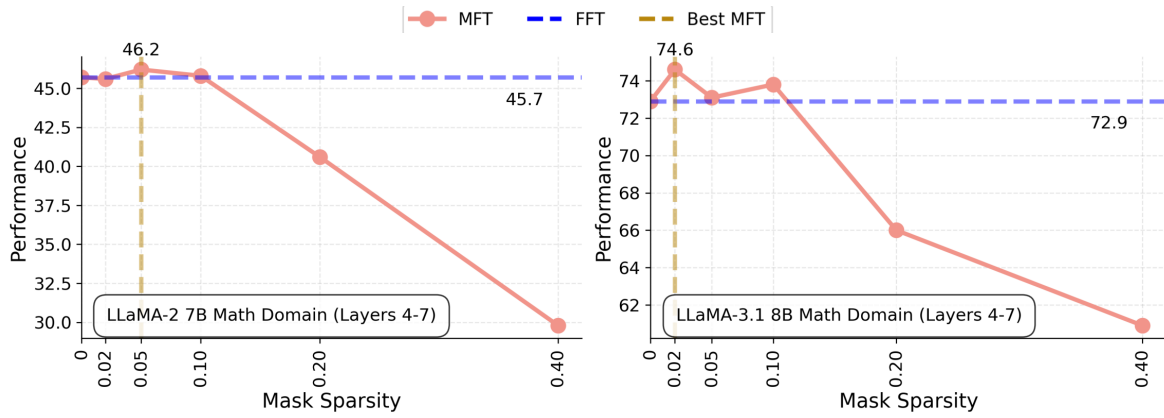


Figure 8. Masking ratio ablation study on math domain using LLaMA2-7B and LLaMA3.1-8B backbones.

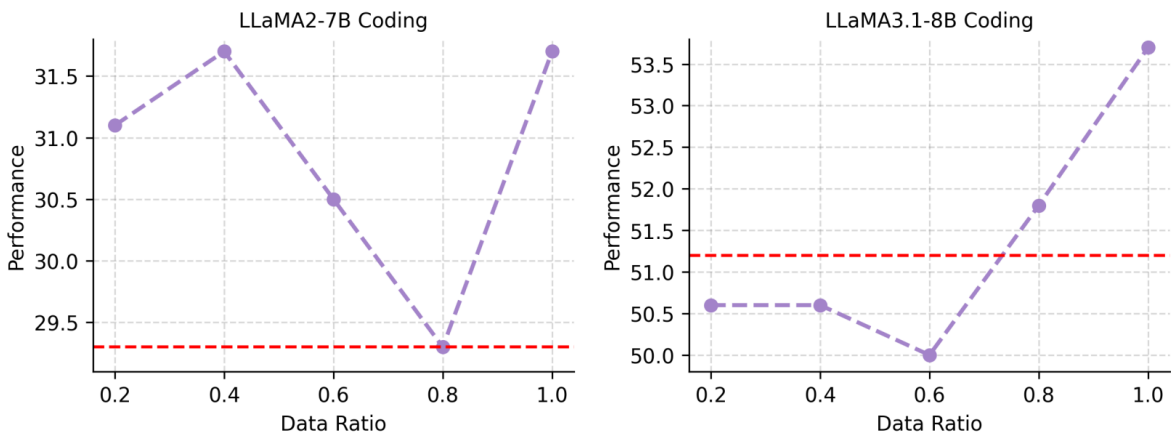


Figure 9. Data ratio ablation study on coding domain using LLaMA2-7B and LLaMA3.1-8B backbones.

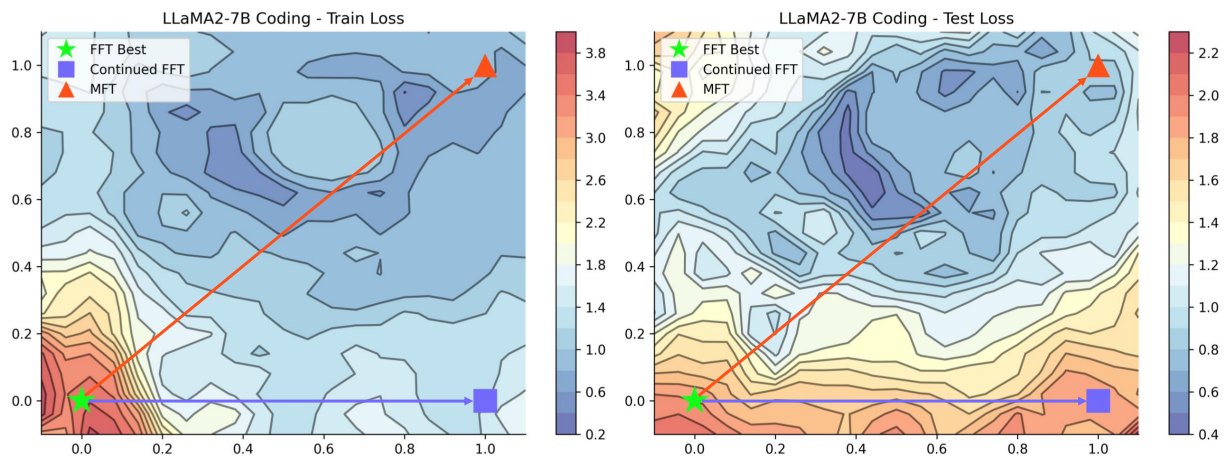


Figure 10. The loss landscape visualization on coding domain using LLaMA2-7B.